

# Confinement of gold quantum dot arrays inside ordered mesoporous silica thin film\*

Chi Yaqing(池雅庆)<sup>1,†</sup>, Zhong Haiqin(仲海钦)<sup>1</sup>, Zhang Xueao(张学骛)<sup>2</sup>, Fang Liang(方粮)<sup>1</sup>,  
and Chang Shengli(常胜利)<sup>2</sup>

(1 School of Computer, National University of Defense Technology, Changsha 410073, China)

(2 School of Science, National University of Defense Technology, Changsha 410073, China)

**Abstract:** Periodic disposed quantum dot arrays are very useful for the large scale integration of single electron devices. Gold quantum dot arrays were self-assembled inside pore channels of ordered amino-functionalized mesoporous silica thin films, employing the neutralization reaction between chloroauric acid and amino groups. The diameters of quantum dots are controlled via changing the aperture of pore channels from 2.3 to 8.3 nm, which are characterized by HRTEM, SEM and FT-IR. UV-vis absorption spectra of gold nanoparticle/mesoporous silica composite thin films exhibit a blue shift and intensity drop of the absorption peak as the aperture of mesopores decreases, which represents the energy level change of quantum dot arrays due to the quantum size effect.

**Key words:** gold quantum dot array; mesoporous silica; quantum size effect; single electron device

**DOI:** 10.1088/1674-4926/30/12/122001

**PACC:** 6416; 7865; 7340R

## 1. Introduction

The synthesis of highly ordered quantum dot arrays has attracted much attention because of their unique structural, optical and electronic properties. These periodic disposed quantum dot arrays could be applied to single electron devices and are very useful in the large scale integration of single electron devices<sup>[1]</sup>. Quantum dots can be assembled from nanoparticles, and the physicochemical properties of quantum dots are highly dependent on the size, shape and arrangement of nanoparticles. Techniques for controlling the structure and organization of quantum dots are strongly desirable. Ordered mesoporous silica thin films are important candidates for the fabrication of highly ordered quantum dot arrays due to their uniform nanopores of various sizes (2–50 nm), shapes (cylindrical and cage-like) and arrangements (lamellar, hexagonal or cubic)<sup>[2–6]</sup>. The pore channels are filled with materials which form quantum dots distributed in ordered nanopores. So it should be possible to control the properties of quantum dots by changing the pore aperture and arrangement of the mesoporous silica thin films.

In most cases, pure mesoporous silica frameworks do not satisfy the synthesis of nanopore-nanoparticle composites because of the weak bonding force between the mesopore host and the nanoparticle guest. Therefore, functionalized mesoporous silica thin films play an important role in the synthesis of highly ordered nanoparticles. The functional group in meso-

porous silica can bond the nanoparticle or the nanoparticle precursor firmly. Up to now, highly ordered nanoparticles of Pt<sup>[7]</sup>, Ag<sup>[8]</sup>, Pd<sup>[9]</sup>, Au<sup>[1,10,11]</sup>, Fe<sub>2</sub>O<sub>3</sub><sup>[12]</sup>, In<sub>2</sub>O<sub>3</sub><sup>[13]</sup>, CdS<sup>[14]</sup>, as well as molybdenum polyoxometalate (PMo)<sup>[15]</sup>, have been synthesized using pure or functionalized mesoporous silica thin films.

In this work, amino-functionalized mesoporous silica thin films were used as host materials to load the gold nanoparticles, employing the neutralization reaction between chloroauric acid (HAuCl<sub>4</sub>) and amino groups<sup>[16]</sup>. The diameters of gold nanoparticles were confined from 2.3 to 8.3 nm when controlling the aperture of pore channels by using three different surfactants, CTAB (Cetyltrimethyl Ammonium Bromide), Brij-56 (C<sub>16</sub>H<sub>33</sub>(OCH<sub>2</sub>CH<sub>2</sub>)<sub>10</sub>OH) and F127 (EO<sub>106</sub>PO<sub>70</sub>EO<sub>106</sub>) as the structure-directing agent. The length-diameter ratios of gold nanoparticles were controlled by adjusting the time limit of the neutralization reaction between the chloroauric acid and the amino group of mesoporous silica. The structures of mesoporous silica are characterized with high resolution transmission electron microscopy (HRTEM), scanning electron microscopy (SEM) and Fourier transform infrared (FT-IR) spectrometry. Ultraviolet-visible (UV-vis) absorption spectra of gold nanoparticle/mesoporous silica composite thin films were observed, which showed an absorption peak around 530 nm due to surface plasma resonance (SPR)<sup>[17]</sup>. The blue shift of the absorption peak was also observed as the aperture of mesopores decreased, which

\* Project supported by the National High Technology Research and Development Program of China (No. 2009AA01Z114), the Advanced Research Foundation of National University of Defense Technology (No. JC08-02-08), and the Innovation Program of National University of Defense Technology for Excellent Postgraduate.

† Corresponding author. Email: yqchi@nudt.edu.cn

Received 25 March 2009, revised manuscript received 25 May 2009

© 2009 Chinese Institute of Electronics

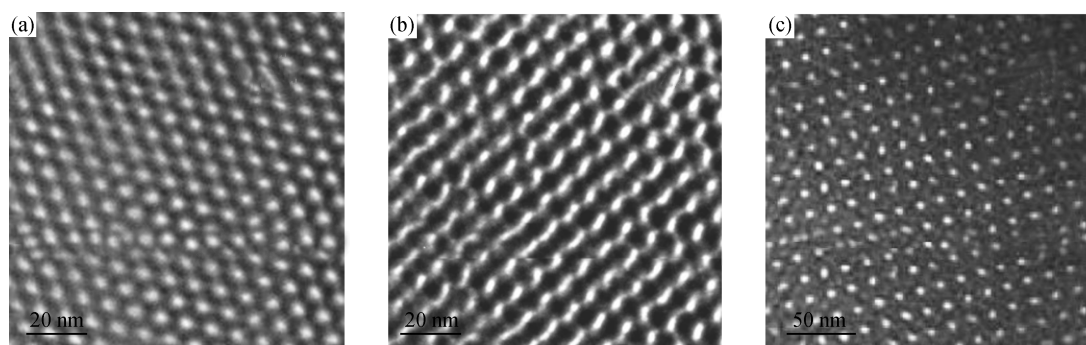


Fig. 1. HRTEM images of amino-functionalized mesoporous silica thin films prepared via (a) CTAB, (b) Brij-56 and (c) F127.

represents the quantum size effect of nanostructures.

## 2. Experimental

### 2.1. Preparation of amino-functionalized mesoporous silica thin film

The preparation of amino-functionalized mesoporous silica films was carried out according to the template-assisted evaporation-induced self-assembly (EISA) procedure applying three kinds of surfactant templates (CTAB, Brij-56 and F127) in order to obtain mesoporous silica thin films with three different apertures. In a typical preparation, the amino-functionalized mesoporous silica thin films are directly synthesized using tetraethoxysilane (TEOS), 3-aminopropyltriethoxysilane (APTES), and surfactant as the silica source, amino-precursor, and structure-directing agent, respectively.

First, TEOS (98%, Aldrich, Milwaukee, WI), ethanol, deionized water and dilute HCl (molar ratios 0.95 : 3.8 : 1 :  $5 \times 10^{-5}$ ) were refluxed at 60 °C for 1 h. The solution was cooled to room temperature and water and concentrated HCl (36%) were added, followed by further ethanol dilution. Next, APTES (99%, Acros, Geel, Belgium) was added slowly to this solution with vigorous stirring at 0 °C to provide amino groups. Then, surfactant was dissolved in ethanol and added to the prehydrolyzed solution. The final reactant molar ratios were 0.95 TEOS : 0.05 APTES : 0.45 HCl : 22 C<sub>2</sub>H<sub>5</sub>OH : 5 H<sub>2</sub>O :  $x$  surfactant, where  $x$  depends on the type of the surfactant. That is,  $x = 0.14$  for CTAB,  $x = 0.082$  for Brij-56, and  $x = 0.006$  for F127. The final solution was stirred for 1 h and aged for another 1 day. Next, the silica/surfactant solution was dip-coated onto silica substrates with a constant withdrawal speed of 50 mm/min. The films were dried in air at room temperature for 1 day and then at 293 K for 1 day. Finally, the surfactant template was removed by extraction with ethanol under reflux at 318 K for 1 day, and the amino-functionalized mesoporous silica thin films were prepared.

### 2.2. Preparation of Au-nanoparticle-loaded mesoporous silica thin film

The Au nanoparticles were assembled into pore channels

of mesoporous silica thin film via a neutralization reaction between chloroauric acid (HAuCl<sub>4</sub>) and the amino group in the pore channels. The diameter of cylindrical Au nanoparticles depends on the aperture of mesopores, while the length of Au nanoparticles could be controlled by the time limit of the neutralization reaction.

First, the silica substrates with fresh amino-functionalized mesoporous silica thin film were dipped into a 0.05M HAuCl<sub>4</sub> aqueous solution for 3 h to fill the Au with the channel. If the reaction lasted over 6 h, the gold nanoparticles would grow out of the channels, even cover the surface of the film and stick the surface too firmly to flush out. Then, the HAuCl<sub>4</sub> outside the channels was flushed away by rapid flow of deionized water. Finally, the composite films were calcined at 400 °C for 3 h under air to obtain gold quantum dot arrays loaded in the pore channels of mesoporous silica thin films.

### 2.3. Characterization

HRTEM images were recorded to observe the surface of mesoporous silica thin films using an FEI Tecnai G2-20 transmission electron microscope operated at 200 kV. SEM images were recorded to observe the cross section of nanopore-nanoparticle composite thin films using a Hitachi S-4800 scanning electron microscope operated at 3.0 kV. FT-IR spectra were obtained using a Nicolet 5700 FT-IR spectrometer with 2  $\mu\text{m}^{-1}$  resolution. Mesoporous silica thin films on the substrates were scratched off and dispersed in KBr powders for FT-IR analysis. UV-vis absorption spectra were recorded on a Hitachi U-4100 spectrophotometer with 2 nm resolution, using air as a reference.

## 3. Results and discussion

### 3.1. HRTEM images

Figure 1 shows representative HRTEM images of amino-functionalized mesoporous silica thin films prepared via CTAB, Brij-56 and F127. The well-ordered characteristic structures confirm the self-assembly effects from three different surfactant templates. The CTAB and Brij-56 dispose the channels hexagonally while F127 disposes them squarely. The aperture also depends on the type of surfactant as well as the

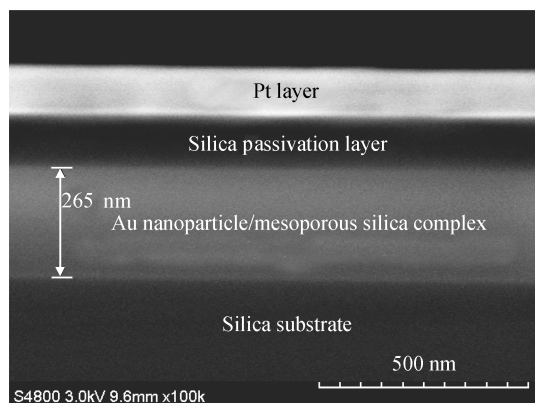


Fig. 2. SEM image of the cross section of Au nanoparticle/mesoporous silica composite thin film.

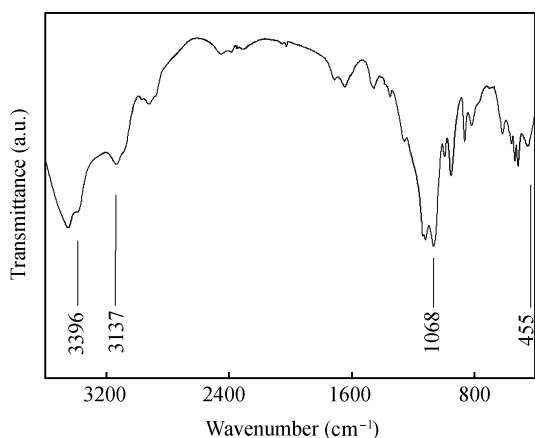


Fig. 3. FT-IR spectrum of amino-functionalized mesoporous silica thin films prepared via F127.

arrangement. The CTAB gives channel apertures around 2.3 nm, the Brij-56 around 3.2 nm, and the F127 around 8.3 nm.

### 3.2. SEM image of cross section

Figure 2 shows a representative SEM image of the cross section of Au nanoparticle/mesoporous silica composite thin film. A nanopore–nanoparticle composite with a thickness of about 265 nm was prepared on the silica substrate. A silica passivation layer was deposited on the composite to protect the ordered mesoporous structure. A platinum layer was deposited on the silica passivation layer to enhance the conductivity of this sample in order to improve the resolution of the SEM image.

### 3.3. FT-IR spectra analysis

Figure 3 shows the FT-IR spectrum of amino-functionalized mesoporous silica thin films prepared via F127. They prove that (a) the signals at 455, 1068 and 3396  $\text{cm}^{-1}$  correspond to the stretching of the Si–O–Si bond in silica; (b) there is no peak at 2870  $\text{cm}^{-1}$  attributed to the F127, showing that surfactant has been well extracted; (c) the peak around 3137  $\text{cm}^{-1}$  can be attributed to the stretching of the N–H bond, which confirms that the  $\text{NH}_2$  groups have been attached to mesoporous silica. The FT-IR spectra of mesoporous silica

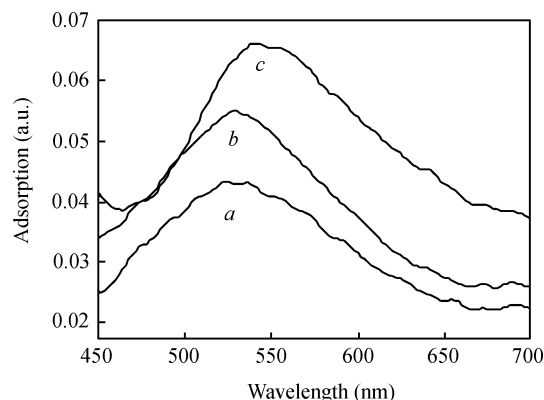


Fig. 4. UV-vis absorption spectra of Au nanoparticles confined by mesoporous silica thin films prepared via (a) CTAB, (b) Brij56 and (c) F127.

thin films prepared via CTAB and Brij-56 show similar phenomena to those via F127.

### 3.4. UV-vis absorption spectra analysis

Figure 4 shows the UV-vis absorption spectra of Au nanoparticles confined by mesoporous silica thin films prepared via CTAB, Brij56 and F127. The blue shift and intensity drop of the absorption peak are clearly observed. When the mesoporous channel aperture decreases from 8.3 to 2.3 nm, the intensity of the absorption peak drops from 0.066 a.u. to 0.043 a.u., and the position of the absorption peak shifts from 538 to 524 nm. The absorption peak of Au confined in mesoporous silica is attributed to surface plasma resonance, and the blue shift and intensity change in the absorption spectrum can be explained in terms of quantum size effects in Au quantum dot arrays.

The surface plasma resonance is due to the collective oscillations of the electron gas at the surface of nanoparticles (6 s electrons of the conduction band for Au nanoparticles), which are correlated with the electromagnetic field of the incoming light<sup>[17]</sup>. Approximately, this resonance is mostly the excitation of the coherent oscillation of the conduction band. So, these absorption peaks provide energy level information on Au quantum dots confined in the mesoporous silica, and the energy gap between the first excited state and ground state  $E_g$  is inversely proportional to the absorption peak, that is  $E_g = \frac{hc}{\lambda}$ , where  $h$  is the Planck constant and  $c$  is the velocity of light.

At the surface of Au nanoparticles, many dangling bonds exist. The smaller the nanoparticle is, the more dangling bonds there are, the higher the electron density of surface is, and the more significant the extension of the electronic wave function outside the nanoparticle surface is. Mie's theory provides a way to calculate the resonance frequency peak  $\omega_S$  of surface plasma resonance<sup>[18]</sup> (equivalent to the peak in UV-vis absorption spectra), that is  $\omega_S = \left[ ne^2 / \epsilon_0 m_{\text{eff}} (1 + \epsilon_b + 2\epsilon_m) \right]^{1/2}$ , where  $n$ ,  $e$ ,  $\epsilon_0$  and  $m_{\text{eff}}$  are the electron density of the nanoparticle, the unit charge, the vacuum permittivity, and the effective mass of the conduction electrons of particles, respectively,  $\epsilon_b$

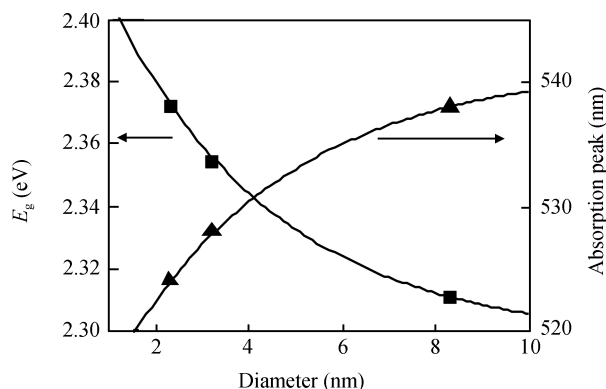


Fig. 5. Energy gap and absorption peak of Au nanoparticles versus the aperture of mesoporous silica.

and  $\epsilon_m$  denote the dielectric constant of the nanoparticle and its host, respectively. So, when the diameter of Au nanoparticles decreases, the electron density of the nanoparticle surface increases, and the blue shift of the peak occurs in the UV-vis absorption spectra. Furthermore, under the same resonance excitation energy, the intensity of the absorption peak drops.

Figure 5 shows the energy gap  $E_g$  and absorption peak  $\lambda$  of Au nanoparticles versus the aperture of mesoporous channels where Au is confined. The square symbols with the fitted curve approximately represent the hyperbolic relationship between the energy gap and the diameter of Au nanoparticles. The energy gap increases with decreasing diameter of Au nanoparticles from 2.31 eV for 8.3 nm to 2.37 eV for 2.3 nm. The triangular symbols with the fitted curve show the blue shift of absorption peaks with decreasing aperture of mesoporous silica, which is consistent with the analysis above.

#### 4. Conclusions

Gold quantum dots with diameters from 2.3 to 8.3 nm are confined inside highly ordered pore channels in amino-functionalized mesoporous silica thin films by using three kinds of surfactant templates (CTAB, Brij-56 and F127), employing the neutralization reaction between chloroauric acid ( $\text{HAuCl}_4$ ) and amino groups. The structures of mesoporous silica thin films are characterized with HRTEM, SEM and FT-IR. UV-vis absorption spectra of gold nanoparticle/mesoporous silica composite thin films exhibit a blue shift and an intensity drop in absorption peak when the aperture of mesoporous channels decreases, which represents the quantum size effect of quantum dots. This synthetic method can be extended to assembly of other metal or semiconductor nanoparticles to obtain ordered quantum dots for the fabrication of single electron devices.

#### References

- [1] Fan H, Yang K, Boye D M, et al. Self-assembly of ordered, robust, three-dimensional gold nanocrystal/silica arrays. *Science*, 2004, 304: 567
- [2] Kresge C T, Leonowicz M E, Roth W J, et al. Ordered mesoporous molecular sieves synthesized by a liquid-crystal template mechanism. *Nature*, 1992, 359: 710
- [3] Inagaki S, Fukushima Y, Kuroda K. Synthesis of highly ordered mesoporous materials from a layered polysilicate. *J Chem Soc Chem Commun*, 1993: 680
- [4] Ogawa M. Formation of novel oriented transparent films of layered silica-surfactant nanocomposites. *J Am Chem Soc*, 1994, 116: 7941
- [5] Inagaki S, Koiwai A, Suzuki N, et al. Syntheses of highly ordered mesoporous materials, FSM-16, derived from kanemite. *Bulletin of the Chemical Society of Japan*, 1996, 69(5): 1449
- [6] Ogawa M. A simple sol-gel route for the preparation of silica-surfactant mesostructured materials. *Chem Commun*, 1996: 1149
- [7] Kumai Y, Tsukada H, Akimoto Y, et al. Highly ordered platinum nanodot arrays with cubic symmetry in mesoporous thin films. *Adv Mater*, 2006, 18(6): 760
- [8] Cai Weiping, Zhang Lide. Synthesis and structural and optical properties of mesoporous silica containing silver nanoparticles. *J Phys: Condens Matter*, 1997, 9: 7257
- [9] Kang H, Jun Y, Park J, et al. Synthesis of porous palladium superlattice nanoballs and nanowires. *Chem Mater*, 2000, 12(12): 3530
- [10] Zhou Lihui, Hu Jun, Xie Songhai, et al. Dispersion of active Au nanoparticles on mesoporous SBA-15 materials. *Chin J Chem Eng*, 2007, 15(4): 507 (in Chinese)
- [11] Shi H, Zhang L, Cai W. Preparation and optical absorption of gold nanoparticles within pores of mesoporous silica. *Mater Research Bulletin*, 2000, 35: 1689
- [12] Fröba M, Köhn R, Bouffaud G.  $\text{Fe}_2\text{O}_3$  nanoparticles within mesoporous MCM-48 silica: *in situ* formation and characterization. *Chem Mater*, 1999, 11(10): 2858
- [13] Yang Haifeng, Shi Qihui, Tian Bozhi, et al. One-step nanocasting synthesis of highly ordered single crystalline indium oxide nanowire arrays from mesostructured frameworks. *J Am Chem Soc*, 2003, 125(16): 4724
- [14] Kouklin N, Menon L, Bandyopadhyay S. Room-temperature single-electron charging in electrochemically synthesized semiconductor quantum dot and wire array. *Appl Phys Lett*, 2002, 80(9): 1649
- [15] Zhang Xueao, Wu Wenjian, Wang Jianfang, et al. Molybdenum polyoxometalate impregnated aminofunctionalized mesoporous silica thin films as multifunctional materials for photochromic and electrochemical applications. *J Mater Res*, 2008, 23(1): 18
- [16] Bharathi S, Lev O. Direct synthesis of gold nanodispersions in sol-gel derived silicate sols, gels and films. *Chem Commun*, 1997, 23: 2303
- [17] Raether H. Surface plasmons on smooth and rough surfaces and on gratings. Berlin: Springer Verlag, 1988
- [18] Kreibig U, Vollmer M. Optical properties of metal clusters. Berlin: Springer Verlag, 1995